LASER INTERFEROMETER GRAVITATIONAL WAVE OBSERVATORY
- LIGO -
CALIFORNIA INSTITUTE OF TECHNOLOGY
MASSACHUSETTS INSTITUTE OF TECHNOLOGY

Technical Note	**LIGO-T2400233–v1**	2024/10/01

Analysis of a Vacuum Beam Guide for Quantum Communications

Hannah Rose

California Institute of Technology
LIGO Project, MS 18-34
Pasadena, CA 91125
Phone (626) 395-2129
Fax (626) 304-9834
E-mail: info@ligo.caltech.edu

Massachusetts Institute of Technology
LIGO Project, Room NW22-295
Cambridge, MA 02139
Phone (617) 253-4824
Fax (617) 253-7014
E-mail: info@ligo.mit.edu

LIGO Hanford Observatory
Route 10, Mile Marker 2
Richland, WA 99352
Phone (509) 372-8106
Fax (509) 372-8137
E-mail: info@ligo.caltech.edu

LIGO Livingston Observatory
19100 LIGO Lane
Livingston, LA 70754
Phone (225) 686-3100
Fax (225) 686-7189
E-mail: info@ligo.caltech.edu

http://www.ligo.caltech.edu/

Contents

1 Abstract

Current solutions for quantum communication channels such as telecom fibers and satellite relays face significant issues such as high loss and disrupted transmission. Huang et al. have introduced a vacuum beam guide as a promising new solution designed to provide a low-loss and stable quantum channel, with less than 10^{-4} dB/km loss not subject to atmospheric variability. This system uses a periodically spaced array of lenses within an evacuated tube to propagate a coherent electromagnetic field over long distances with minimal loss. The initial proposal is limited to analyzing a confocal vacuum beam guide and calculates only absorption loss and a preliminary estimate of alignment loss. Our analysis further examines the performance of a generalized class of vacuum beam guide configurations with the inclusion of physical imperfections using computer optics simulations. These simulations were developed into software tools that allow for detailed evaluation and optimization of different vacuum beam guide configurations. By identifying a configuration's alignment tolerances, this work enables the development of a system that is suitably insensitive to realistic constraints. These results advance the vacuum beam guide closer to potential implementation as a quantum communication channel and contribute to the realization of reliable, continental-scale quantum communications with low loss and high throughput.

2 Introduction

Covering the globe with a system of quantum communication would allow for large developments in information security by implementing quantum cryptographic key distribution [1], precision distributed measurement by the use of non-local coherences [2] and transmission of entangled information [3], and broadly a realization of the "quantum internet" with the connection of physically separated quantum nodes [4]. However, prior to the successful implementation of a large-scale quantum network, reliable, low-loss, long-distance quantum channels must be engineered capable of transporting the quantum information over the network without corruption or loss of coherence. The optical channel requires a significantly higher quality than those utilized for classical communication due to the limitations of quantum error correcting codes when compared to their classical counterparts [5]. Current demonstrations of quantum transmission typically involve transmission of the quantum information in light over optical channels such as fiber [6][7] or transmission via satellites [8][9]. The use of optical fiber is relatively cheap and simple to implement, but suffers from high loss at long distances, with a typical attenuation on the order of $0.2\,\mathrm{dB\,km^{-1}}$ due to the constant interaction with the fiber. Transmission via satellite relay networks shows comparatively low absorption due to the inter-satellite links occurring in vacuum but suffers instead from the challenges of relaying the signal through the atmosphere to an orbiting train of satellites. As a result, communications rely on fair weather and retain a loss on the order of 30 dB from the diffraction and attenuation of the beam while transmitting through the lower atmosphere. Given these limitations, a hybrid approach merging vacuum transmission with a rigid, ground-based channel, the vacuum beam guide shows promise.

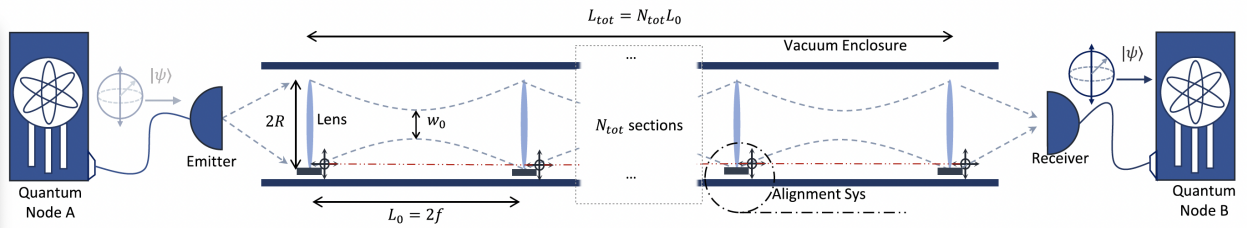

Figure 1: The vacuum beam guide proposed by Huang *et al*

3 Vacuum Beam Guide for Quantum Communications

Utilizing technology developed for the laser interferometer gravitational wave observatory (LIGO) interferometers, Huang *et al* propose a vacuum beam guide as a state-of-the-art channel for long-distance quantum communications [10]. As depicted in Fig 1, the vacuum beam guide would consist of a periodic array of lenses to support a periodic Gaussian mode of transmission, repeatedly refocusing the beam to reduce the maximum diameter of the beam and thereby the necessary encompassing tube. To reduce the total amount of absorption of the beam in matter, the beam tube is held at vacuum and the lenses are kept sparse in the tube. Appropriate mode matching at the input and output of the beam guide is then responsible for interfacing the beam with the optical setups at both ends. The system is predicted to allow for optical transmission with attenuation due to absorption, diffraction, and misalignment on the order of $10^{-4}\,\mathrm{dB\,km^{-1}}$ for reasonable parameters and consequentially a channel capacity on the order of 10^{13} Qubits/s over 10^{4} km. If implemented, this quality of connection would exceed the current fiber-based communication by orders of magnitude. This work aims to further the understanding of the vacuum beam guide by programmatically simulating and assessing the transmission of squeezed light stated through an optimized vacuum lens array using the Finesse3 optics simulation package developed to model interferometric gravitational wave detectors [11]. This allows for the incorporation of more realistic noise sources, such as the scattering of the transmission beam into higher-order Hermite-Gaussian modes and the surface imperfections of physical lenses, as well as assessing the effects of noise-mitigation systems such as serrated baffles.

In this analysis, the vacuum beam guide is modeled paraxially as a periodic series of thick lenses, each 3 cm thick with a 1.444 index of refraction as preliminary values. For simplicity, the radii of curvature on both sides of the lens are kept equal. Although a realistic implementation of the vacuum beam guide would involve turns and steering mirrors to avoid obstacles and correct the beam trajectory, here the beam guide is modeled as a straight path without active control to determine the stability of the system to natural imperfections and misalignments. Ignoring reflections, these thick lenses can be equated to ideal thin lenses with a slightly altered separation by equivalence of their ABCD matrices. This periodic series of lenses is then equivalent to periodic transmission in a resonant cavity [12], allowing any stable resonator configuration to generate an equivalent stable vacuum beam guide configuration. For a beam guide with all-identical lenses considered here, this equates to a symmetric cavity, but asymmetric two-mirror cavities or multi-mirror cavities could be equated to vacuum beam guides with alternating or cycling patterns of lenses. This work focuses on the matching lens configuration due to its simplicity both in the number of vary-

Focal Scale	0.70	0.75	0.78	0.80	1.00	1.25	1.40	1.50
Waist at Focus [cm]	2.42	2.56	2.60	2.68	3.04	3.37	3.52	3.62
Waist at Lens [cm]	4.53	4.43	4.40	4.37	4.30	4.35	4.39	4.43
Rayleigh Range [km]	1.19	1.33	1.38	1.45	1.88	2.30	2.52	2.65
Divergence Angle [µrad]	20.4	19.3	18.9	18.4	16.2	14.7	14.0	13.6

Table 1: Symmetric Vacuum Beam Guide Solutions

ing parameters and bulk manufacturing as well as the fact that an asymmetric lens array would result in unequal spot sizes of the transmitting mode on the lenses. As the size of the encasing tube is dictated by the largest of the spot sizes, it is likely beneficial to utilize this size at all lenses. This symmetric cavity then has a stability criterion for the focal scale, the ratio of the focal length of the mirrors or lenses to their separation:

$$f_{scale} = f/L \geq \frac{1}{4} \tag{1}$$

This family of solutions is parameterized fully by the focal scale, the separation between lenses, and the number of repeated segments, or equivalently the focal scale, the number of repeated segments, and the total length of the vacuum beam guide. From this family, eight focal scales were chosen to investigate, using an arbitrary 3.75 km segment length and transmitting at a 1550 nm wavelength, as shown in Table 1. The radius of the lenses is 12 cm with full absorption outside this circle. These include the confocal, $f_{scale} = 1$ design proposed by Huang et al. [10] as well as the $f_{scale} = 0.78$ design found by parameter optimization [13]. The $f_{scale} = 1.40$ design was included to match the waist size on the lens of the $f_{scale} = 0.78$ design, and the other solutions were included to show the effect of slight variations away from these solutions.

4 Simulation Work

To evaluate the performance of the vacuum beam guide with these configurations, the system was modeled in the Finesse3 optical simulation software [11]. This Python package allows for the construction of a model out of elementary optical elements such as curved interfaces and spacers and the simulation of a coherent source of laser light or squeezed vacuum propagating through the optics and being measured by a series of detectors. The calculations are performed by propagating the specified source Gaussian beam through the system according to the ABCD matrices. Astigmatism of the Gaussian beam is constrained to align to the x-y axes of the model. The effects of apertures, small misalignments, and lens imperfections are calculated by expressing the electromagnetic field between components as a two-dimensional Hermite-Gauss expansion to finite order and then determining the coupling caused between the different ingoing and outgoing components. The models can then be evaluated both for the losses and scattering of a Gaussian beam in transmission and the squeezing transmitted through the system as a model of quantum data transmission. For the classical characterization, a laser element is introduced at the input of the beam guide with the appropriate Gaussian mode. A series of detectors are then placed throughout the beam guide and at

the output to measure the power in the middle and end of the guide and the scattering of power into higher-order Hermite-Gaussian modes. For the quantum characterization, a simulated homodyne detector interferes the squeezed vacuum with a local oscillator, and the reduction in the quantum noise from the squeezed vacuum is measured. This is performed in the simulation both prior to entering the vacuum beam guide and after exiting the beam guide to measure the reduction in squeezing due to transmission losses.

First, the vacuum beam guide was simulated as a perfectly aligned series of perfect lenses, with losses only resulting from the aperture clipping at each lens and the absorption and reflections at each lens. For each lens 6 ppm of the light was absorbed, and 3 ppm of the light was reflected off of each surface of each lens. To consider this best-case scenario, the $f_{scale} = 0.78$ configuration was tested as it had been optimized for this ideal case. Eighty segments were included for a total 300 km, over which the vacuum beam guide has a loss of only 1900 ppm or 0.008 dB, 2.7×10^{-5} dB/km. Additionally, the transmitted beam remains strongly in the fundamental Gaussian mode, with a fraction of the light scattering into higher modes, visually similar to the Laguerre-Gauss $p = 1, l = 0$ mode, seen in Fig 2. With 22 dB of input squeezing, the output of the beam guide was measured to retain 20.8 dB of squeezing on the output of the beam guide, surpassing the theorized 20.5 dB conservative upper limit for fault-tolerant squeezed-light quantum computing [14]. We can compare this with a theoretical value for squeezing reduction by pure attenuation as calculated in [15],

$$S = S_0(1 - l) + l \tag{2}$$

where S_0 is the initial fractional amount of squeezing and l is the fractional loss in the system. This also predicts a reduction to 20.8 dB output squeezing, with an insignificant deviation attributable to phase error.

Then, to investigate the effects of real lens imperfections and misalignments a rough phase map was applied to the lenses, and each lens was offset and tilted randomly. Optimally, a vacuum beam guide design would be sufficiently robust to misalignments to not require costly professional installation of each lens. The phase maps were randomly generated from $1/f$ spatial frequency noise as shown in Fig. 3 and applied to both sides of each lens, with each phase map being independently generated. Then lens tilts and offsets were added to the simulation space parameterized by the standard deviation of the misalignments. The misalignments in both axes for both tilt and offset of each lens were taken independently from identical Gaussian distributions with the specified variance, modeling alignment errors that are entirely uncorrelated. In Finesse3, lens tilts are natively supported as parameters, but offsets in the transverse plane are not supported. Instead, offsets have been implemented as a offset of the aperture map and an equivalent tilt of the lens. The equivalent lens tilt can be determined from equating the optical path length through the tilted lens and the offset lens as a function of tangential displacement. In one dimension this looks like for a curved interface

$$OPD_{tilt} = (n_2 - n_1)\left[\frac{x^2}{2R} - x\theta\right] \tag{3}$$

$$OPD_{offset} = (n_2 - n_2)\frac{(x - \Delta)^2}{2R} = (n_2 - n_1)\left[\frac{x^2}{2R} - x\frac{\Delta}{R} + \frac{\Delta^2}{2R}\right] \tag{4}$$

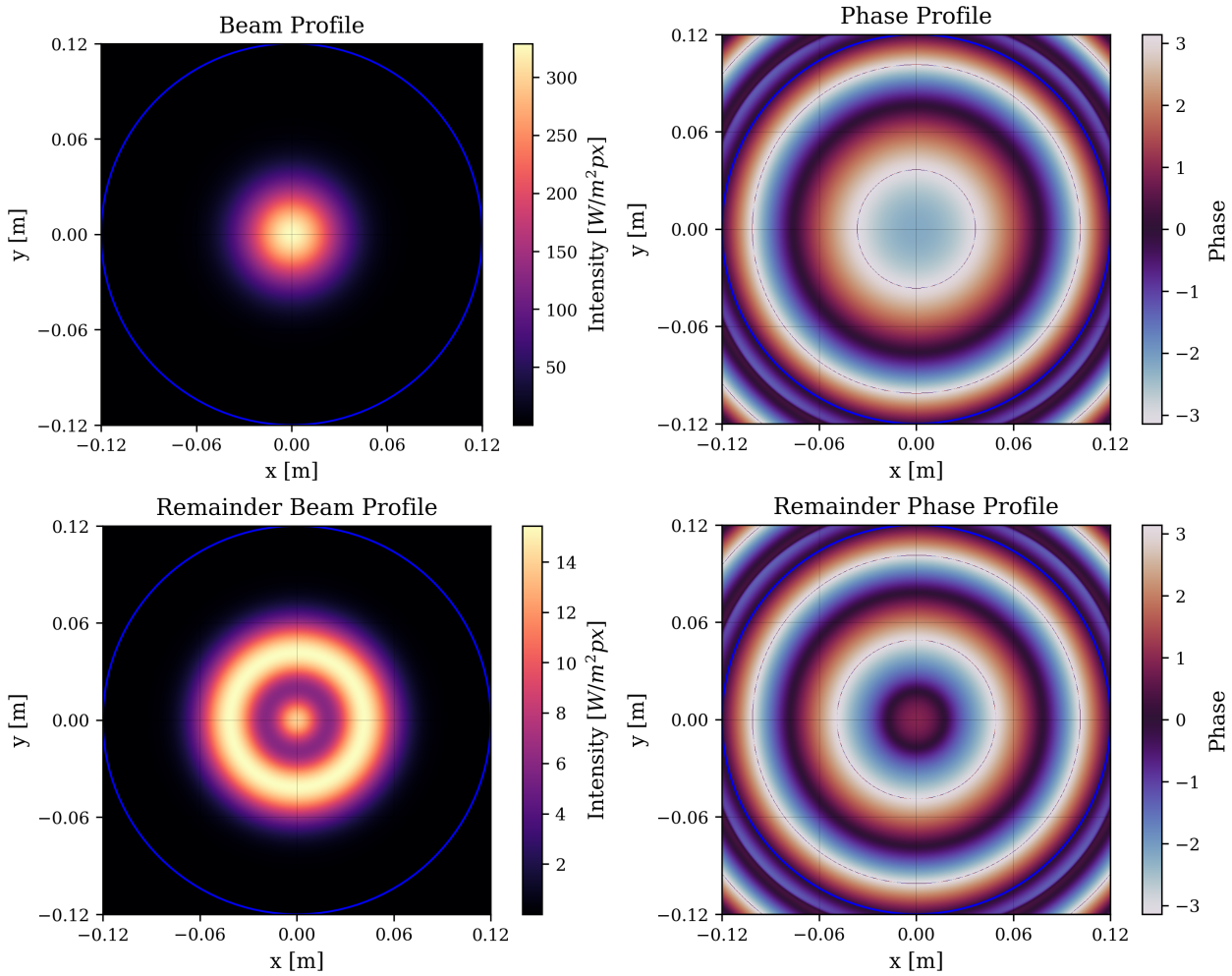

Figure 2: For the aligned $f_{scale} = 0.78$ configuration, the intensity and phase maps of a 1 W Gaussian beam immediately prior to the 10th lens, alongside the same plots with the fundamental Gaussian mode subtracted out.

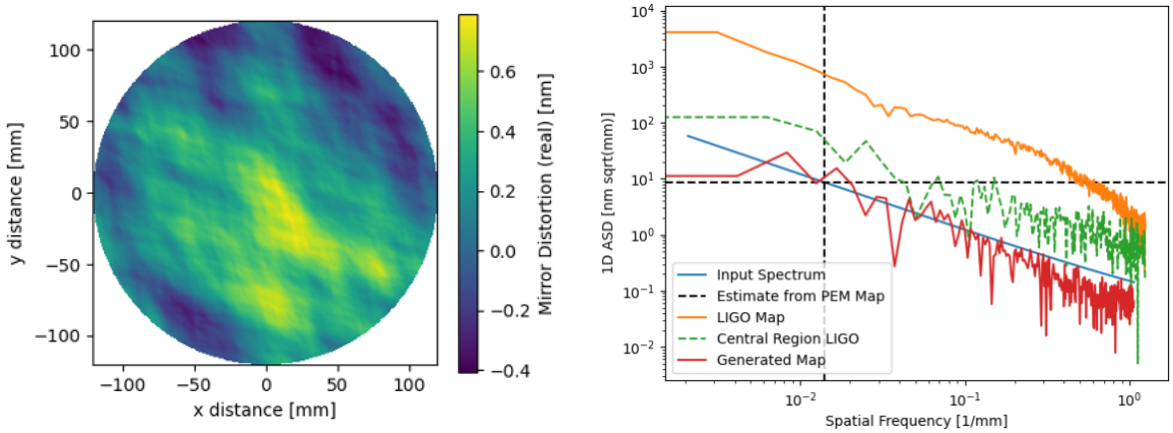

Figure 3: A characteristic phase noise map alongside the amplitude spectral density of its cross-section.

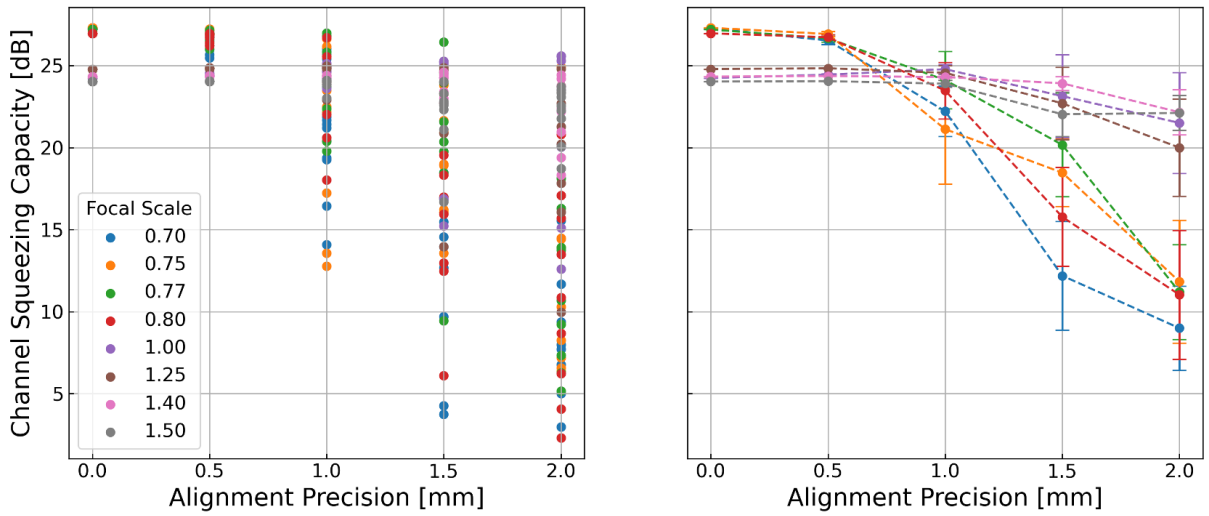

Figure 4: The channel capacity of each beam guide generated with a given offset standard deviation (left) alongside the same summarized into the average for each focal scale with 2σ error bars (right). 300 km total length in 80 3.75 km segments.

yielding an equivalence in the linear terms

$$\theta \sim \frac{\Delta}{R} \tag{5}$$

This allows the implementation of a transverse offset in Finesse3 up to the paraxial approximation. For this approximation to hold, the tilts of the lenses must remain significantly smaller than the divergence angle of the Gaussian beam being modeled, here tens of microradians. Due to the large radius of curvature, a one-millimeter offset equates to less than one microradian of tilt for all of the modeled configurations, so substantial offsets of up to a centimeter can be modeled.

With each of several offset variances for each configuration, several lens arrays were generated, each with independent misalignments and the same 80 lens segments, and the total power transmitted was measured. The loss was then converted to a channel squeezing capacity

$$S_{max} = -10 \cdot \log l \tag{6}$$

given by the maximum squeezing output allowed under Eq. 2. As the effect of phase corruption on the output squeezing was not significant in the aligned case and the output beam profiles computed for the misaligned cases were largely consistent with astigmatic Gaussians, this figure can be considered a good estimate for the capacity of the vacuum beam guide configurations. The results of these simulations with perfect tilt alignment are shown in Fig. 4. As expected, channel capacity decreases with increasing misalignments, and as misalignments become large, there is an increasing probability of a very low channel capacity as the beam becomes more likely to exit the window of the apertures. This data also shows a significant distinction between solutions with focal scales greater and less than one in that focal scales greater than one have significantly lower channel capacities when perfectly aligned but remain more resilient to misalignments resulting in a superior channel capacity for misalignments of 1 mm or more. The abruptness of this transition merits further investigation to

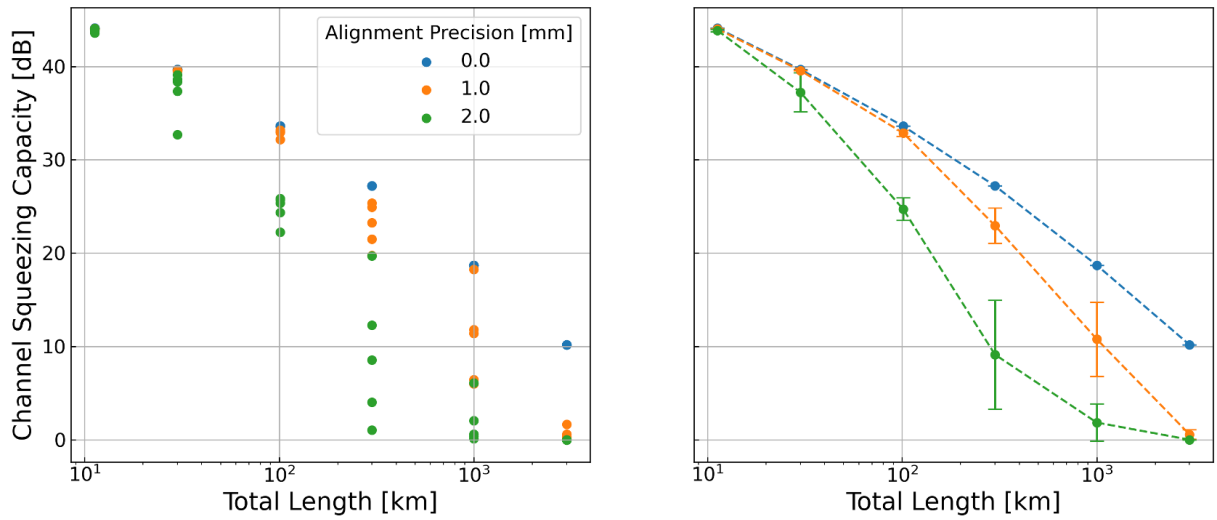

Figure 5: The channel capacity of each beam guide generated with a given length (left) alongside the same summarized into the average for each length with 2σ error bars. $f_{scale} = 0.78$, 3.75 km segments

validate and explain the effect to ensure that it does not result from a simulation artifact. To test how this loss scales with distance, the $f_{scale} = 0.78$ solution was simulated with a varying number of 3.75 km segments. Again, the lenses were given random surface textures and offsets, with the resulting channel capacities shown in Fig. 5. The loss increases faster than linearly with distance, potentially indicating compounding errors as the beam propagates through the beam guide, and for the 2 mm misaligned beam guides, transmission abruptly drops to zero, again as the beam begins to travel outside of the windowed apertures.

The modeling of tilt misalignments is somewhat more difficult. Given the small divergence angle, the tens of microradian tilts that can be modeled within the paraxial approximations are vanishingly small compared to what is feasible without costly precision alignment of the lenses. As an attempt to measure the sensitivity of the system to tilts, the $f_{scale} = 0.70$ configuration was modeled with varying tilt alignment precisions less than the divergence angle, as shown in Fig. 6. As tilt distributions up to ten microradians showed no significant effects to the losses in the beam guide and Finesse3 is currently unable to natively model larger tilts in the x and y planes simultaneously, an alternative approach is required to assess vacuum beam guides for resilience to these alignment errors. The Finesse3 beamsplitter object allows for tilts larger than the divergence angle by calculating the outgoing beam direction and astigmatism, but due to Finesse3 restricting the astigmatism to the x-y axes, any given beamsplitter can only model a tilt in one of these axes. Therefore, a simulation of larger tilts would require either estimating the three-dimensional result from a two-dimensional simulation or utilizing an optical simulation system based on more general astigmatic Gaussian beams such as IfoCAD [16].

Additionally, for tilts that are larger than the divergence angle yet still sufficiently small, the effects of the lens misalignments can be modeled as introducing deviations into the path of the outgoing beam. To consider the effects of the optics on the path of a ray using the ABCD matrix formalism, the ray can be transformed onto the axis of the optic, propagated

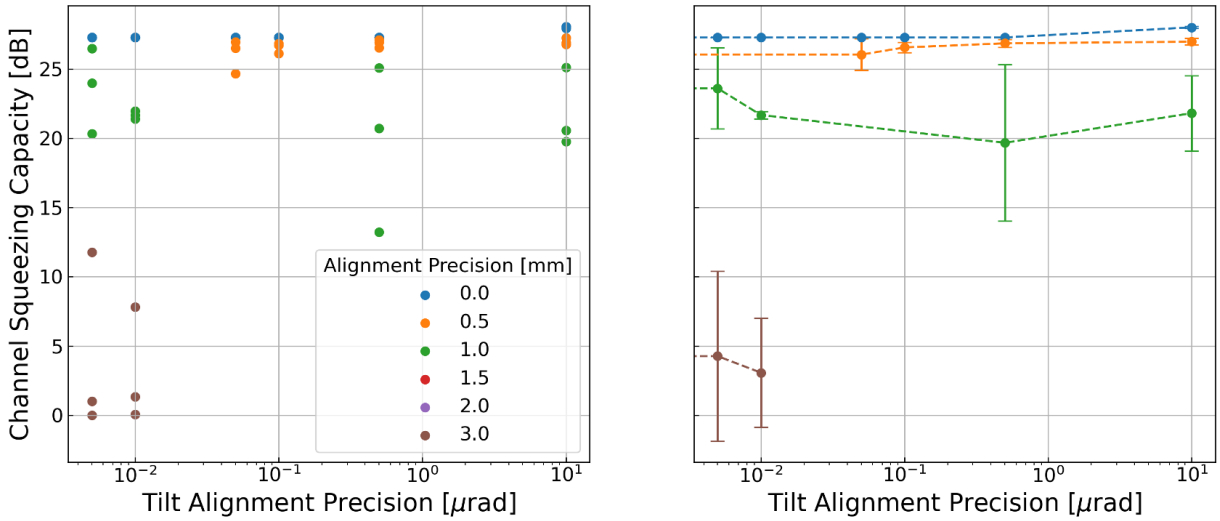

Figure 6: The channel capacity of each beam guide generated with a given tilt alignment precision (left) alongside the same summarized into the average for each precision with 2σ error bars. $f_{scale} = 0.70$, 300 km total length in 80 3.75 km segments.

through the optic, and then transformed back into the original frame. For a lens with offset δ_{lens} and tilt β_{lens}, the displacements to the outgoing ray offset δ_{ray} and angle β_{ray} are then given as

$$\begin{bmatrix} \delta_{ray} \\ \theta_{ray} \end{bmatrix} = \begin{bmatrix} A-1 & B \\ C & D-1 \end{bmatrix} \begin{bmatrix} \delta_{lens} \\ \theta_{lens} \end{bmatrix} \tag{7}$$

Although this model would fail to capture the astigmatism of the Gaussian beam generated by the misalignments, utilizing this model to calculate the location of the apertures relative to the beam path could allow a moderately accurate simulation of significant two-dimensional lens tilt misalignments within the Finesse3 model.

5 Conclusions

The vacuum beam guide provides for ultra-low loss quantum transmission over continent-scale distances. Using Finesse3, solutions can be examined for losses and resilience against realistic imperfections. To this effect, solutions with focal scales less than one differ sharply from those with focal scales greater than one, having higher aligned capacities while being more sensitive to displacements. The effects of lens surface imperfections are rather simple to implement, with more analysis to be performed to determine maximum roughness constraints. Simulation of realistic tilt misalignments is rather more difficult in Finesse3 and will require an alternative approach to direct implementation in Finesse3. Additionally, the Finesse3 simulation should be checked with varying truncations of Hermite-Gauss modes to ensure convergence and compared against other optical simulation packages such as SIS and OSCAR to ensure that the system is being accurately modeled.

Additionally, the vacuum beam guide should be modeled for transient noise sources akin to the glitches occurring in LIGO data. As the vacuum beam guide must span large distances,

the system will likely need to cross high-noise environments that could vibrate or jostle the lenses. Due to the pre-existing connected land ownership, it would be convenient for the vacuum beam guide to travel adjacent to railroad lines, requiring insusceptibility to such large, prolonged noise. This could require the addition of serrated baffles between lenses to block the off-axis scattered light from interfering with the primary beam.

If realized, the vacuum beam guide would allow not only for large quantum key distribution but also distributed quantum precision measurements. Strong entanglement would allow the synchronization of atomic clocks [6] between cities, allowing for the measurement of gravitational time dilation as an analog of geologic mass movements [17]. A sharing of quantum states between interferometers could improve the combined sensitivity of a network of gravitational wave observatories through the reduction of noise sources [2]. In the optical spectrum as well, the sharing of entangled states can provide for an interferometric combination of multiple observatories for vastly increased angular resolution [3]. By linking detectors, the ability to entangle noise and compare results prior to measurement allows for superior sensing [18].

6 Acknowledgments

This work was supported by the National Science Foundation Research Experience for Undergraduates (NSF REU) program, the LIGO Laboratory Summer Undergraduate Research Fellowship program (NSF LIGO), the California Institute of Technology Student-Faculty Programs, and the Thomas Lauritsen Named SURF Fellowship. Special thanks go to my mentors for this work, Rana Adhikari and Aaron Goodwin-Jones, as well as my fellow SURF Prakhar Maheshwari.

References

[1] Feihu Xu, Xiongfeng Ma, Qiang Zhang, Hoi-Kwong Lo, and Jian-Wei Pan. Secure quantum key distribution with realistic devices. *Reviews of Modern Physics*, 92(2):025002, May 2020. Publisher: American Physical Society.

[2] Marco Malitesta, Augusto Smerzi, and Luca Pezzè. Distributed quantum sensing with squeezed-vacuum light in a configurable array of Mach-Zehnder interferometers. *Physical Review A*, 108(3):032621, September 2023. Publisher: American Physical Society.

[3] Daniel Gottesman, Thomas Jennewein, and Sarah Croke. Longer-Baseline Telescopes Using Quantum Repeaters. *Physical Review Letters*, 109(7):070503, August 2012. Publisher: American Physical Society.

[4] H. J. Kimble. The quantum internet. *Nature*, 453(7198):1023–1030, June 2008. Publisher: Nature Publishing Group.

[5] Nicolas Sangouard, Christoph Simon, Hugues de Riedmatten, and Nicolas Gisin. Quantum repeaters based on atomic ensembles and linear optics. *Reviews of Modern Physics*, 83(1):33–80, March 2011. Publisher: American Physical Society.

[6] K. Predehl, G. Grosche, S. M. F. Raupach, S. Droste, O. Terra, J. Alnis, Th. Legero, T. W. Hänsch, Th. Udem, R. Holzwarth, and H. Schnatz. A 920-Kilometer Optical Fiber Link for Frequency Metrology at the 19th Decimal Place. *Science*, 336(6080):441–444, April 2012. Publisher: American Association for the Advancement of Science.

[7] M. Schioppo, J. Kronjäger, A. Silva, R. Ilieva, J. W. Paterson, C. F. A. Baynham, W. Bowden, I. R. Hill, R. Hobson, A. Vianello, M. Dovale-Álvarez, R. A. Williams, G. Marra, H. S. Margolis, A. Amy-Klein, O. Lopez, E. Cantin, H. Álvarez Martínez, R. Le Targat, P. E. Pottie, N. Quintin, T. Legero, S. Häfner, U. Sterr, R. Schwarz, S. Dörscher, C. Lisdat, S. Koke, A. Kuhl, T. Waterholter, E. Benkler, and G. Grosche. Comparing Ultrastable Lasers at 7×10^{-17} Fractional Frequency Instability Through a 2220 Km Optical Fibre Network. *Nature Communications*, 13(1):212, January 2022. Publisher: Nature Publishing Group.

[8] Juan Yin, Yuan Cao, Yu-Huai Li, Sheng-Kai Liao, Liang Zhang, Ji-Gang Ren, Wen-Qi Cai, Wei-Yue Liu, Bo Li, Hui Dai, Guang-Bing Li, Qi-Ming Lu, Yun-Hong Gong, Yu Xu, Shuang-Lin Li, Feng-Zhi Li, Ya-Yun Yin, Zi-Qing Jiang, Ming Li, Jian-Jun Jia, Ge Ren, Dong He, Yi-Lin Zhou, Xiao-Xiang Zhang, Na Wang, Xiang Chang, Zhen-Cai Zhu, Nai-Le Liu, Yu-Ao Chen, Chao-Yang Lu, Rong Shu, Cheng-Zhi Peng, Jian-Yu Wang, and Jian-Wei Pan. Satellite-based entanglement distribution over 1200 kilometers. *Science*, 356(6343):1140–1144, June 2017. Publisher: American Association for the Advancement of Science.

[9] Sheng-Kai Liao, Wen-Qi Cai, Wei-Yue Liu, Liang Zhang, Yang Li, Ji-Gang Ren, Juan Yin, Qi Shen, Yuan Cao, Zheng-Ping Li, Feng-Zhi Li, Xia-Wei Chen, Li-Hua Sun, Jian-Jun Jia, Jin-Cai Wu, Xiao-Jun Jiang, Jian-Feng Wang, Yong-Mei Huang, Qiang Wang, Yi-Lin Zhou, Lei Deng, Tao Xi, Lu Ma, Tai Hu, Qiang Zhang, Yu-Ao Chen, Nai-Le Liu, Xiang-Bin Wang, Zhen-Cai Zhu, Chao-Yang Lu, Rong Shu, Cheng-Zhi Peng, Jian-Yu Wang, and Jian-Wei Pan. Satellite-to-ground quantum key distribution. *Nature*, 549(7670):43–47, September 2017. Publisher: Nature Publishing Group.

[10] Yuexun Huang, Francisco Salces–Carcoba, Rana X. Adhikari, Amir H. Safavi-Naeini, and Liang Jiang. Vacuum Beam Guide for Large Scale Quantum Networks. *Physical Review Letters*, 133(2):020801, July 2024. Publisher: American Physical Society.

[11] Daniel Brown, Samuel Rowlinson, Sean Leavey, Philip Jones, and Andreas Freise. Finesse3, July 2024.

[12] Steven J. M. Habraken and Gerard Nienhuis. Modes of a twisted optical cavity. *Physical Review A*, 75(3):033819, March 2007. Publisher: American Physical Society.

[13] Prakhar Maheshwari. LIGO-T2400254-v1: Vacuum Beam Guide for Quantum Communication, July 2024.

[14] S. Takeda and A. Furusawa. Toward large-scale fault-tolerant universal photonic quantum computing. *APL Photonics*, 4(6):060902, June 2019.

[15] Aaron Jones, Ricardo Cabrita, Mikhail Korobko, Martin van Beuzekom, Daniel Brown, Viviana Fafone, Joris van Heijningen, Alessio Rocchi, Mitchell Schiworski, and Matteo

Tacca. Supplementary document for Transverse Mode Control in Quantum Enhanced Interferometers: A Review and Recommendations for a New Generation - 6793088.pdf. February 2024. Publisher: Optica Publishing Group.

[16] Evgenia Kochkina. Stigmatic and astigmatic Gaussian beams in fundamental mode. July 2013.

[17] J. Müller, D. Dirkx, S. M. Kopeikin, G. Lion, I. Panet, G. Petit, and P. N. A. M. Visser. High Performance Clocks and Gravity Field Determination. *Space Science Reviews*, 214(1):5, November 2017.

[18] Zheshen Zhang and Quntao Zhuang. Distributed quantum sensing. *Quantum Science and Technology*, 6(4):043001, July 2021. Publisher: IOP Publishing.